The EMPIR initiative is co-funded by the European Union's Horizon 2020 research and innovation programme and the EMPIR Participating States

EMPIR 16ENG03 HyMET
Project title: Hybrid Metrology for thin films in energy applications

Deliverable D2: **Best practice guide for measurement and data analysis of complex thin film (mixed-phase samples) using a combination of metrological methods including optical reflectometry. The guide will cover the definition of the required reference samples as well as the procedure for determination of optical measurement accuracy in order to increase relevance to industrial quality control**

Lead partner: BAM
Contributing partners: PTB, TUB, VSL, CMI, Accurion, CEA
Due date: September 2019
Submission date: December 2019

This guide consists of page 1 to 18 and has no supplements

Reference: HyMET (EMPIR-ENG 53)

Authors: Andreas Hertwig[1], René Sachse,
Vasile-Dan Hodoroaba

Bundesanstalt für Materialforschung und -prüfung
Unter den Eichen 87
12205 Berlin

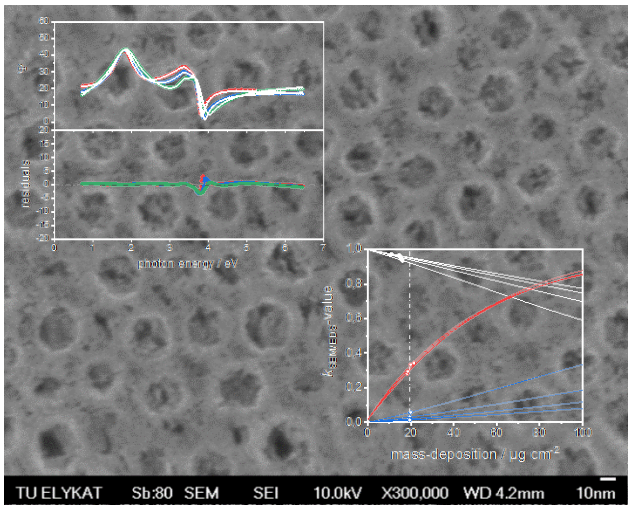

Thisdocument is a Best Practice Guide developed by BAM and partners for the HyMET project.

https://www.hymet.ptb.eu

The EMPIR initiative is co-funded by the European Union's Horizon 2020 research and innovation programme and the EMPIR Participating States

[1] Author for correspondence.
Andreas Hertwig, Bundesanstalt für Materialforschung und -prüfung, Unter den Eichen 44 – 46, 12203 Berlin, Germany
andreas.hertwig@bam.de

Introduction

Regarding the rising energy demand and the imminent climate change, the development of a sustainable, fossil-free fuel and chemical production become of global importance. One possible goal is the development of electrochemical conversion processes using catalysts. The complex morphology of suitable catalysts constitutes a challenge even for modern analytical techniques and requires new approaches employing the combination/complementation of data of different analytical methods. Among the materials used in energy technology, mesoporous metal oxides are one of the most interesting because of their wide-spread application as catalysts, electrodes, battery components, but also because of the challenges they present for analytical methods. Their key parameters are layer thickness, porosity, mixing ratio of the metals in case of mixed metal layers, the in-depth distribution of the chemical composition, electrical conductivity, and electrocatalytical activity. Here, we show a methodology for a multi-sample analysis of mesoporous mixed oxide thin layers. As an example, we chose mixed oxides of TiO_2 and IrO_2 used as electrode coatings on the anode side of electrocatalytic water splitting reactors (oxygen evolution reaction) [1, 2]. This is a mesoporous system already quite well understood recently, but very difficult for all analytical methods employed. It can be prepared with large variances of the properties and is in principle accessible to a range of different analytical methods, such as electron and optical microscopies or X-ray spectroscopy.

Measurement methodologies covered in this guide

This guide covers the determination of the layer thickness, porosity, and elemental composition for mixed mesoporous layers of metal oxides. As an example, mixtures of TiO_2 and IrO_2 have been investigated extensively within the HyMET project. Within this guide, we concentrate on analysing the mesoporous layer samples by means of three different analytical methods:

1. Spectroscopic ellipsometry (SE) for obtaining layer thicknesses, oxide dielectric function, and porosity out of one single experiment. From the oxide dielectric function, the composition of mixed oxides can be obtained as explained later.
2. Scanning electron microscopy (SEM) in top-view, cross-section and transmission mode for visualising the surface morphology and obtaining the layer thickness; further, in combination with energy-dispersive x-ray spectroscopy (EDX) the elemental composition can be extracted.
3. Electron-probe microanalysis with EDX analysis for obtaining the mixing ratio of the oxides, the mass-deposition as well as the density of the layer, providing an alternative way to determine the porosity.

Figure 1 shows a possible collection of methods usable for mesoporous layers with their respective advantages and disadvantages. A good analysis strategy shall try to obtain as much useful data as possible while keeping in mind the measurement and analysis expense. Here, we try to aim for a methodology benefiting the most for production purposes. This is achieved by developing spectroscopic ellipsometry analysis as a production-friendly

technique, but with the strong metrological advantages of other methods for improved and quantified accuracy.

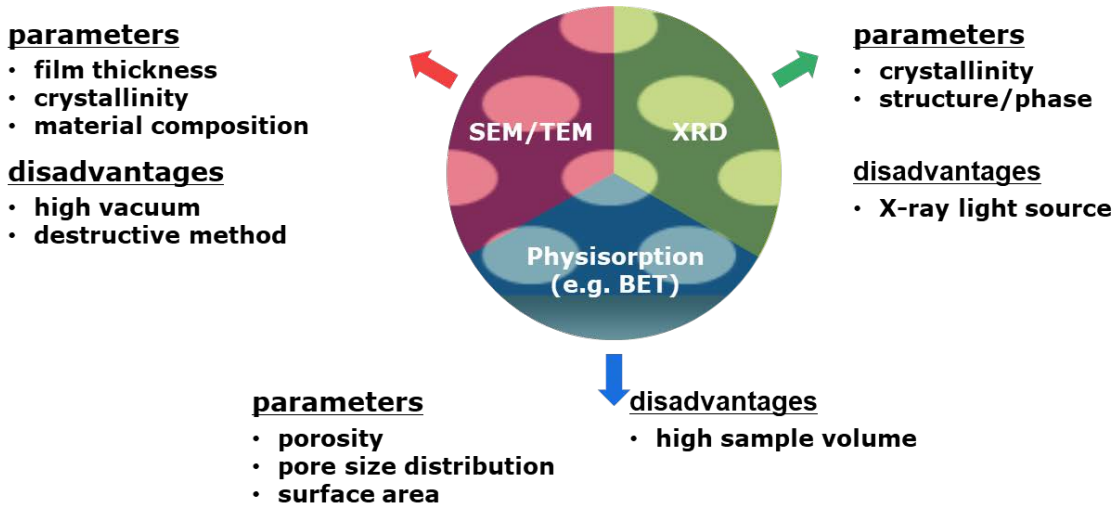

Figure 1: Overview over some possible analysis methods usable for complex mesoporous layers.

Spectroscopic Ellipsometry

Ellipsometry is a specular reflection spectroscopic technique with polarised light [3-5]. It relies on the fact that phase information can be obtained from an optical reflection experiment if the polarisation information is measured. The complex reflection coefficient is then

(1) $$\rho = \frac{r_p}{r_s} = \tan(\Psi) \cdot e^{i\Delta},$$

where r_p and r_s are the Fresnel reflection coefficients for p- and s-polarisation, tan(Ψ) is the amplitude ratio of the electrical field, and Δ is the phase difference of the p and s wave (parallel and perpendicular to the plane of incidence), respectively. Ellipsometry, together with related methods like X-ray reflectometry, is a very useful technique to analyse surfaces and thin layers.

The main advantage is that it is generally non-destructive, fast, and scalable, therefore in situ and in-line capable. There is, however a disadvantage to this type of methods: The analysis of the spectra of Ψ and Δ is normally achieved with a model-based strategy as shown in Figure 2. The most important parameter in this analysis is the figure of merit. In our case, we use the root mean squared error, RMSE,

(2) $$RMSE = \sqrt{\frac{1}{2U-\mathrm{V}+1}\sum_{i=1}^{U}\left[\left(\frac{\Psi_i^{mod.}-\Psi_i^{exp.}}{\sigma_{\Psi_i}^{exp.}}\right)^2+\left(\frac{\Delta_i^{mod.}-\Delta_i^{exp.}}{\sigma_{\Delta_i}^{exp.}}\right)^2\right]},$$

with the number of measured data points U, the number of fit parameters V, the model and experimental values of the ellipsometric parameters Ψ^{mod}, Ψ^{exp}, Δ^{mod}, Δ^{exp}, respectively, and the experimental uncertainties for these values, $\sigma_{\Psi_i}^{exp.}$ and $\sigma_{\Delta_i}^{exp.}$. This parameter serves as a measure of fit quality and plays a very important role in the determination of the model-based uncertainty (see below).

This means that all the relevant parameters are only obtained indirectly as the results of a fit process. Therefore, a combination strategy using different methods and comparing the results for better accuracy (cross-method metrology) as well as establishing a common model with which to analyse different measurement results (hybrid metrology) should prove useful for complex layer measurement tasks in the future.

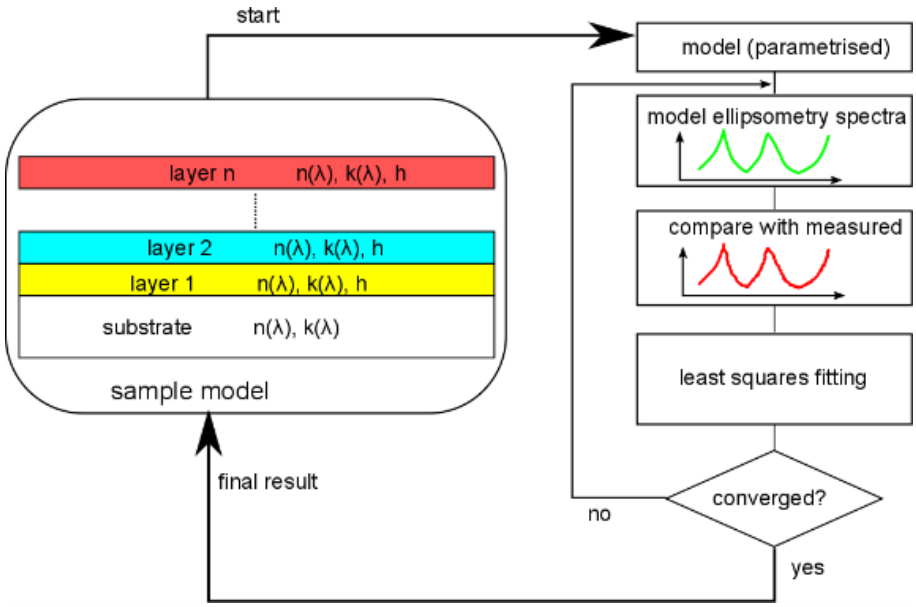

Figure 2: Analysis scheme of spectroscopic ellipsometry. n(λ), k(λ): optical constants of the layers, h: layer thickness.

In this study, apart from the standard analysis methodology of ellipsometry for ideal layers, we have employed the BEMA (Bruggeman effective medium analysis) for taking into account mixtures of different oxides and a-BEMA (anisotropic BEMA) for handling the geometrically anisotropic optical constants / dielectric function of the porous layer [6]. The effective dielectric responses ε in this model can be calculated as

(3) $$\sum_{n=1}^{m} f_n \frac{\varepsilon_n - \varepsilon_{eff,j}}{\varepsilon_{eff,j} + L_j(\varepsilon_n - \varepsilon_{eff,j})} = 0,$$

(4) $$L_j = \frac{U_x U_y U_z}{2} \int_0^\infty \frac{\left(s+U_j^2\right)^{-1} ds}{\sqrt{\left(s+U_x^2\right)\left(s+U_y^2\right)\left(s+U_z^2\right)}},$$

with the volume fractions f_n, the bulk-like dielectric functions ε_n, the effective dielectric functions $\varepsilon_{eff,j}$, as well as the ellipsoidal form factors U_x, U_y, and U_z. This model includes a quantitative treatment of the anisotropy from the fact that the voids in our case are not sphere-shaped, but ellipsoidal. While the quantitative information gained from the depolarisation factor in the a-BEMA model is not very accurate for our samples and will not be treated further here, it provides a check for the validity of the assumptions about the structure of the layers.

The total setup of the layer composition is then as depicted in Figure 3. The layer consists of a mixture of oxide and void. The oxide in turn consists of a mixture of two different metal oxides.

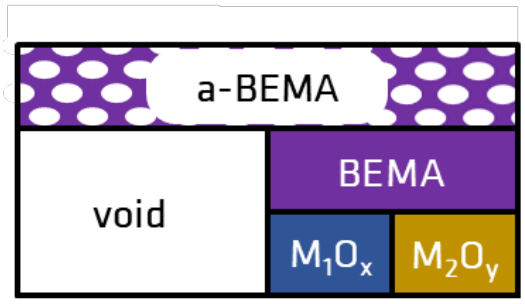

Figure 3: Analysis strategy for mixed oxide mesoporous layers with a double effective material approach.

Apart from this use of the effective medium approach (EMA) for analysing mixed phases, we have used two additional modelling techniques to improve the accuracy of the ellipsometric analysis:

1. Using multi-sample analysis, we can combine the measured data of many different samples where the properties vary among the samples. For example, we can vary the layer thickness or the porosity or both in combination itself leaving if possible, all other parameters the same. This will insert restrictions into our modelling, as the properties of the layer material (without the influence of the changed parameters) should stay the same. This can be observed by merging the data and reflecting the multi-sample property of the analysis in the model. This is an especially strong method to enhance the accuracy. It can increase the amount of useful data per modelling run by several orders of magnitude.
2. For the analysis of strongly absorbing materials such as IrO_2, we use a method called resonance enhancement. We deposit the layer on top of a silicon substrate with a thermal oxide layer as an in-between buffer layer. This increases the contrast towards the absorbing layer. In parallel, the sensitivity of the analysis towards the optical constants will increase. This is normally used for analysing thin metallic layers, but we will use it here because pure IrO_2 is almost metallic in its properties.

All results shown in this guide were obtained by means of combining these measurement and modelling methods to the largest possible extent: We analysed layers of the oxides with different values for the layer thickness and the porosity on bare silicon substrates with only the native oxide (~2 nm in thickness) present. We then did the same using oxidised substrates with nominal oxide thicknesses of 150 nm and 1000 nm, respectively. This is the general procedure we recommend for the ellipsometric analysis when dealing with this task.

The data of many of these samples were combined and analysed in a multi-sample analysis scheme. Each ellipsometric measurement was performed in a wavelength range of 192 nm – 1697 nm with a Woollam M2000DI instrument using angles of incidence (AOI) from 50° to 80° with steps of 5°. The data analysis was done with the CEASE ellipsometry analysis software. However, this guide as well as the normative texts cited here are intended to be fully equipment-neutral. We do not endorse any specific brand or version of instruments or software to use.

Generally, it is desirable to have many AOI values, but sample inhomogeneity may cause the results to vary with the angle. It is strongly recommended to check for this effect while using the method described here.

Preparation of samples

The preparation of different layers containing a mixture of TiO_2 and IrO_2 is now well-established in literature [2]. In short description, we use a templated sol gel synthesis via EISA (evaporation induced self-assembly) mechanism depicted schematically in Figure 4 in the general case of the mixed oxide. For a detailed analysis of the chemistry of this process and the chemical and electrochemical properties of the resulting layers, please refer to [1]. Generally, the amount of voids inside the layer (the porosity filling factor in %) is achieved by varying the template concentration in the solution before dip-coating, drying and calcination. With this parameter, we have achieved the porosity to be variable over a very large range. Further, we have achieved that this process is compatible with variations of the layer chemistry determined by the sol composition.

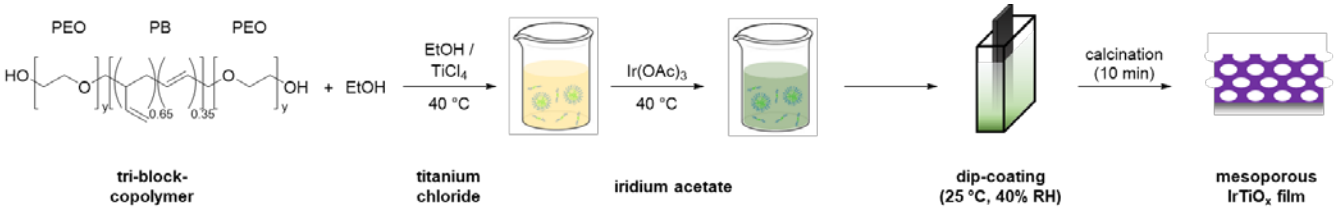

Figure 4: Schematic chemical synthesis if the mesoporous mixed oxide layers.

Electron microscopy and EPMA (EDS)

Electron probe microanalysis (EPMA) means the chemical identification and quantification of very small amounts of substance (<0.1 pg) when the sample is excited with an electron beam and the emitted characteristic X-rays are analyzed. It relies on an interaction between the electrons and the sample, which leads to ionization with emission of electrons from the inner electron shell followed by emission of X-rays. The chemical (elemental) identification and quantification can be carried out either by means of energy-dispersive X-ray spectrometry (EDS) or wavelength-dispersive X-ray spectrometry (WDS) by using a scanning electron microscope (SEM).

The quantification of the mass-depositions (in µg cm^{-2}) based on the model originated from the work of Pouchou and implemented in the thin-film analysis software package StrataGem.[7] The program iteratively fits calculated $k_{SEM/EDS}$-values of X-ray lines to the measured $k_{SEM/EDS}$-values, whereas mass deposition and elemental composition are set as unknown parameters. $k_{SEM/EDS}$-values are the ratio of the X-ray intensity of the element to be examined in the unknown sample to the X-ray intensity of the same element in a sample of known elemental concentration (standard ore reference sample). In order to obtain a good fit of the measured $k_{SEM/EDS}$-values, three to four different electron beam acceleration voltages are necessary. It should be noted that the acceleration voltage must be chosen in

a way that all elements in the layer and the substrate are identified in the X-ray spectra with an acceptable signal-to-noise ratio.

The analysis software StrataGem converts the mass-deposition into a film thickness by known film density. For the determination of film porosities, the inverse way is used by measuring the film thickness from cross-sectional SEM imaging and dividing the calculated mass-deposition by the film thickness. Average film porosities can then be calculated by considering the density of a bulk (non-porous) material (e.g. IrO_2 = 11.66 g cm^{-3}).[8] The overall EPMA approach is illustrated in Figure 5.

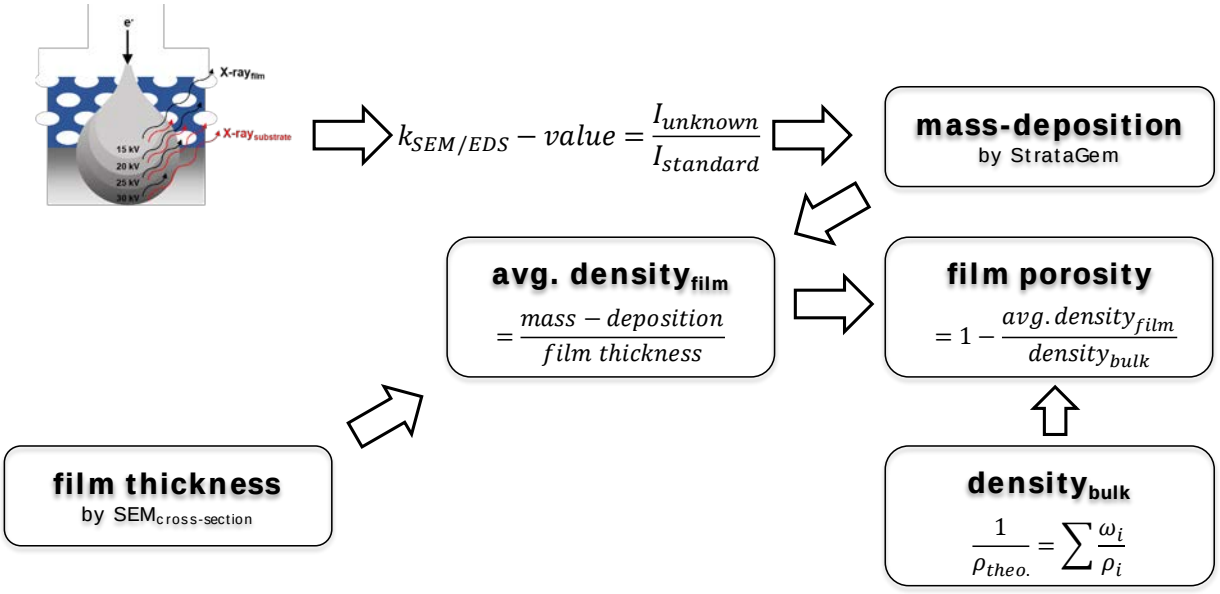

Figure 5: Schematically illustration of the EPMA approach for the determination of film porosities.

Example results for pure TiO_2

Electron microscopy

In this section, the multi-method analysis of porous thin layers is described through the example of pure TiO_2 layers. This methodology is later expanded to pure IrO_2, and then to mixed $Ti_xIr_{1-x}O_2$ layers. Figure 6 shows the different SEM images from which the SEM analysis is derived. An overview (left image) confirms the mesoporous layer structure and shows the distribution of the voids in the layer. The voids self-organise to some extent taking roughly a closest packing of ellipsoids but without long-range order. The HR-SEM (high-resolution SEM) (centre image) shows the morphology of the voids. This is important in many cases as high calcination temperatures can lead to prominent changes in the layer structure, sometimes shrinking the voids by migration and crystallization.

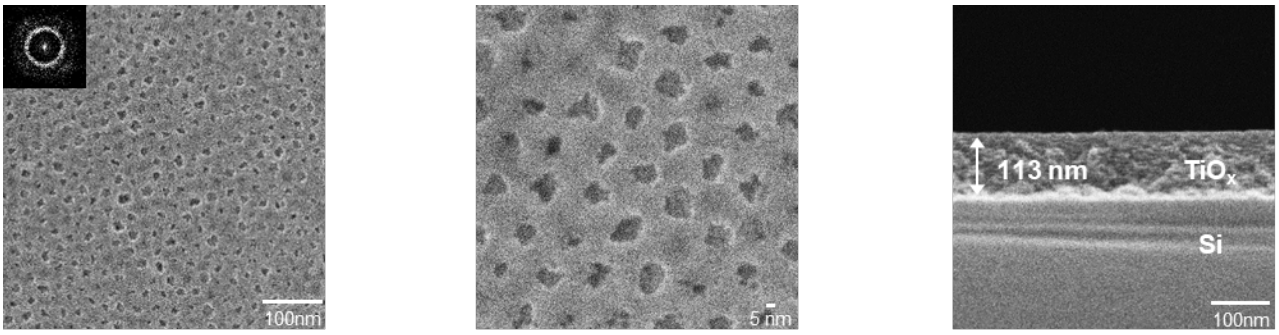

Figure 6: SEM analysis of a pure TiO_2 sample in the versions used for this work. Left: overview image with an inserted 2D Fourier transform showing the degree of order of the voids, centre: hig-resolution image to evaluate the void morphology and shape, right: cross section view with inserted measurement of the layer thickness.

The layer thickness can be determined by SEM on cross-sectioned samples (in this case 113 nm). All cross sections discussed here are obtained by mechanically breaking the samples. Other techniques, like ion beam milling have been shown in the past to introduce too many artefacts (e.g. curtaining) [8].

EPMA

Figure 7 displays the results of the EPMA approach and the determination of the mass-deposition by the StrataGem software from a mesoporous titanium oxide film on a silicon substrate. For the analysis, four acceleration voltages (15, 20, 25, 30 kV) were applied on three different areas (200x200 µm^2). $k_{SEM/EDS}$-values (circles) are calculated from the X-ray intensities of the unknown TiO_2 sample and X-ray intensities of a pure TiO_2 standard with known concentration. These $k_{SEM/EDS}$-values are iteratively fitted by the StrataGem Software (curves in the left plot) and the elemental composition as well as the mass-deposition (right plot; in this case 19.5 µg cm^{-2}) of the film are calculated. With the film thickness from cross-sectional SEM imaging, the average density of the film can be extracted and related to the density of bulk TiO_2 to obtain the porosity of the film.

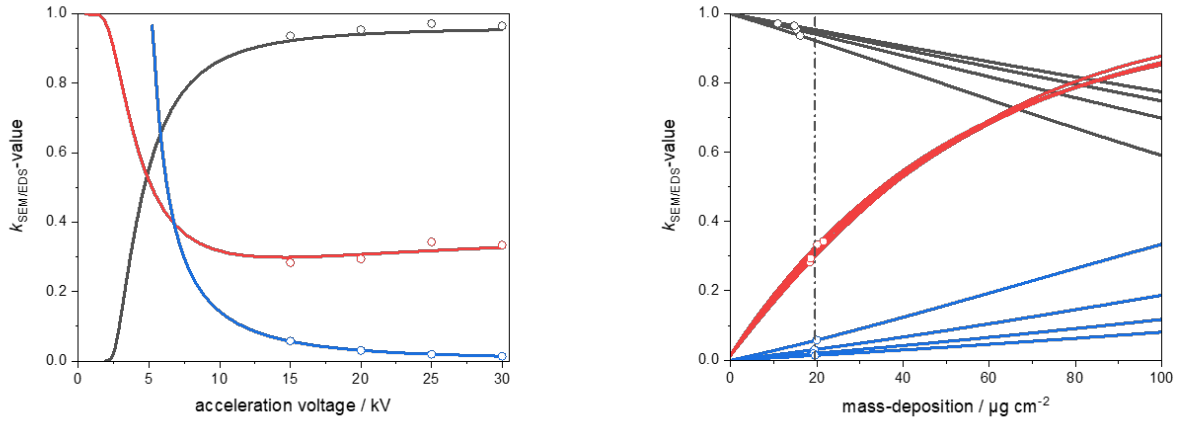

Figure 7: EPMA analysis of a thin mesoporous TiO_2 film on a silicon substrate.

Spectroscopic Ellipsometry

Figure 8 shows an example of an SE analysis performed on a pure TiO_2 sample. Shown are the results of the measurement in Ψ and Δ along with the values obtained by the fit. Using the methods described in [8, 9] and according to the methods described in [10], we depict the measurement and fit curves together with the residuals of the measurement. While the fit quality is generally regarded as very good for this type of analysis, we have to accept some residual mismatch which is due to the complexity of the model. The residuals and the RMSE value of the fit are in this case not good enough to quantify the accuracy of the measurement. We have to do a sensitivity analysis as described in the last section of this guide.

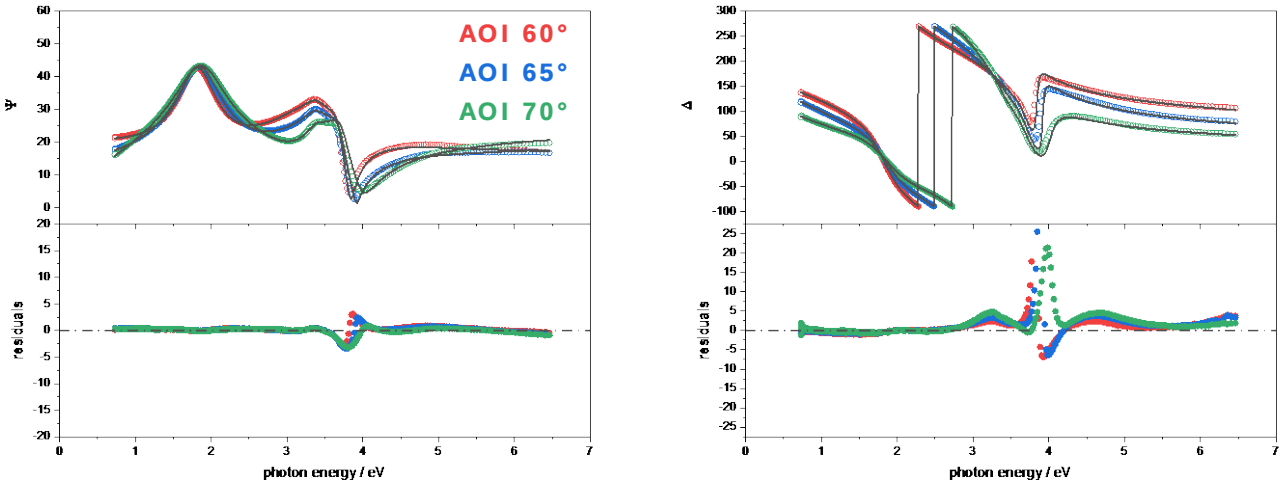

Figure 8: Results of a typical spectroscopic ellipsometry experiment on a pure TiO_2 sample.

Figure 9 and Figure 10 show parity plots (cross-method comparison between SE and electron microscopy analysis) for a larger number of samples. Figure 9 compares the layer thickness obtained from SE with the values resulted from the geometrical analysis of the SE images. Figure 10 does the same for the film porosity obtained from SE and from EPMA.

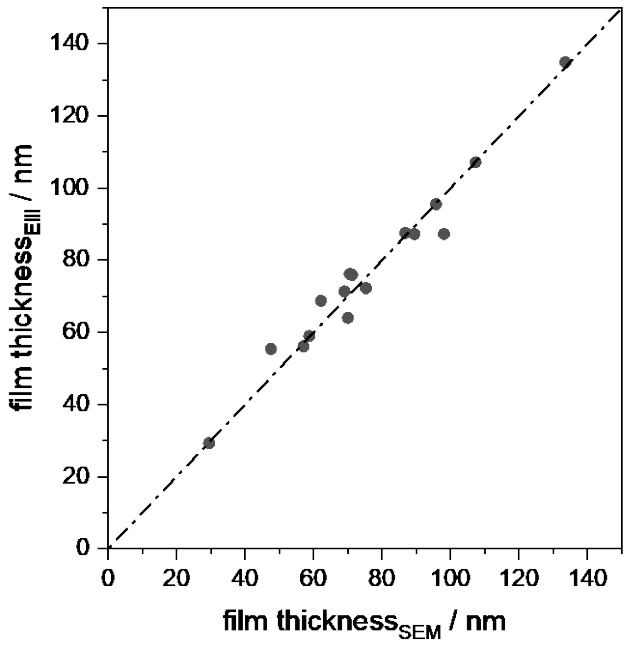

Figure 9: Parity plot comparing thickness values from SE (Elli) and SEM for different pure TiO_2 layers.

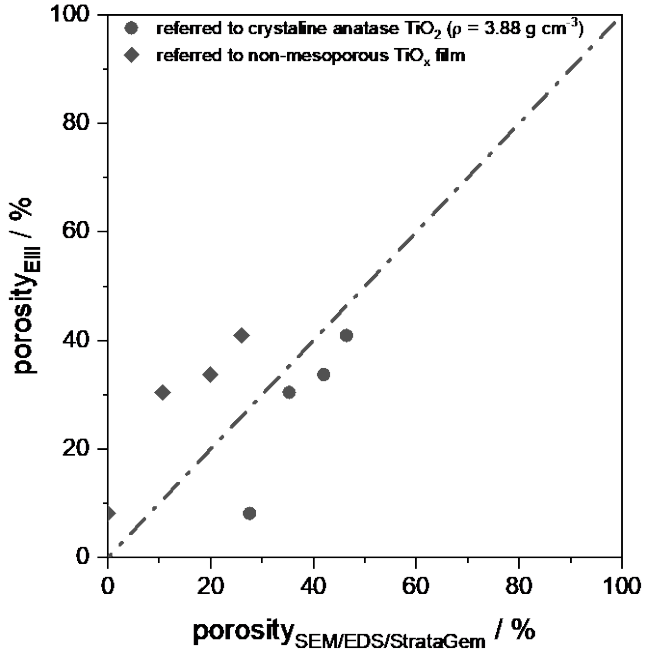

Figure 10: Parity plot comparing values for the porosity for different pure TiO_2 layers.

It is obvious that the agreement between the techniques is reasonably good in the case of the layer thickness. This is a confirmation of the models used in the analysis. In the case of the porosity values, the agreement becomes somewhat less good. The reasons behind this behaviour are currently still under investigation. As a working theory, we see the main reason in the assumption of a layer material density when performing the EPMA analysis. This is the one crucial point where EPMA relies on a piece of information from other methods that is not obtainable with reasonable effort. It is to our knowledge not possible to produce the oxides discussed here in a solid layer completely without micro- or mesoporosity. Simply omitting the template will not result in such a layer or in a layer similar to the ones produced by vapour deposition and related methods. Such layers would be needed as reliable references to make this analysis complete. Therefore, we will always deal with some degree of uncertainty in the EPMA. Nevertheless, these results constitute a striking proof of the effectiveness of the present method. Further, the quantification of the low-energy X-ray line of oxygen (525 eV) is not as reliable as for lines of higher energies such as Ti Kα (4.5 keV). The EPMA quantification in the present study has been performed by working with Ti Kα and setting the film stoichiometry as TiO_2.

Example results for pure IrO_2

As of now, there is still not enough well-analysed data available on pure IrO_2 layers to give a full account on the porosity analysis in the case of pure IrO_2. However, we have used the case of pure IrO_2 to develop a good optical model for this material which is presented here.

SEM analysis

Figure 11 shows the result of a SEM analysis pure iridium oxide. As can be seen, we obtain the same morphology of the layer and the voids on the surface as for the TiO_2 case. The film thickness can be readily obtained from the SEM images on cross-sectioned samples.

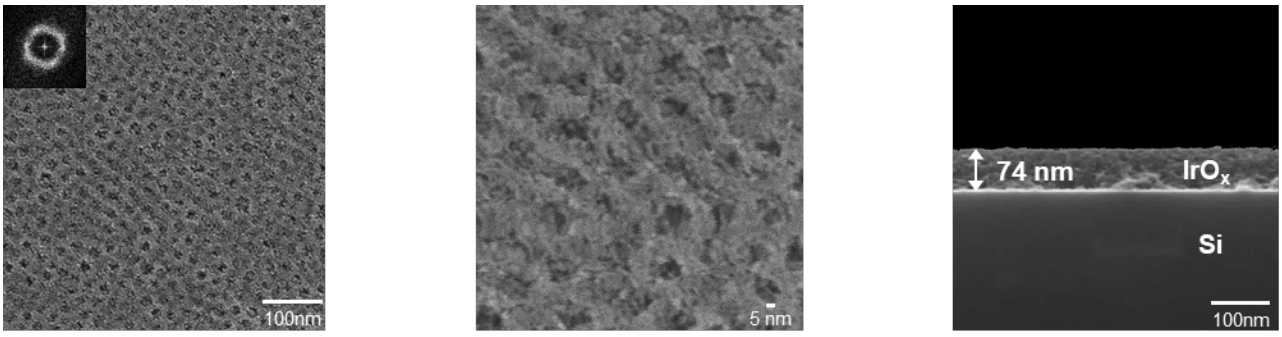

Figure 11: SEM analysis of a pure IrO_2 layer.

SE analysis of pure iridium oxide

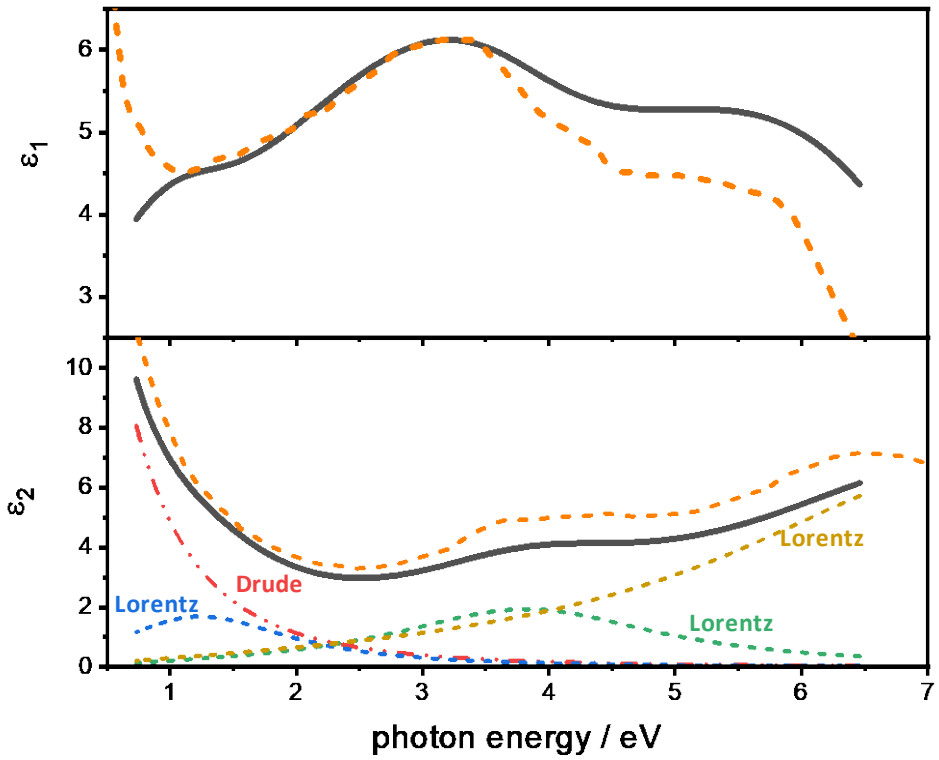

Figure 12: Dielectric function, real (ε_1) and imaginary part (ε_2) of pure IrO2, deconvolution and comparison: Black: The dielectric function. Red: Drude component, Yellow: UV Lorentz peak, Green: Vis Lorentz peak, Blue: Near-IR Lorentz peak, Orange: comparison dielectric function for sputtered IrO_2 from [11].

Figure 11 shows the dielectric function obtained from SE. As the layers are highly conductive the presence of a Drude part in the spectrum is expected. We have managed to describe the measurement data well enough by only adding three absorption bands on top of the Drude edge, one in the near IR, visible, and UV. The UV Lorentz component can be seen as indicating a band edge which is hidden by the other absorption bands within the dielectric function. In the figure we show a comparison of IrO_2 with literature data from the work of Choi et al. [11] on sputtered IrO_2. The agreement with this work based on theory and Kramers-Kronig analysis is reasonably well to confirm our hypothesis that our layers consist of pure iridium oxide and that our version of IrO_2 shows a typical optical response for this material.

Example results for mixed oxides

In this example, like before, we have to prove that the overall morphology of the synthesised layers is as assumed. Again, SEM image analysis confirms the presence of the voids and yields the thickness of the oxide layer, as shown in Figure 13.

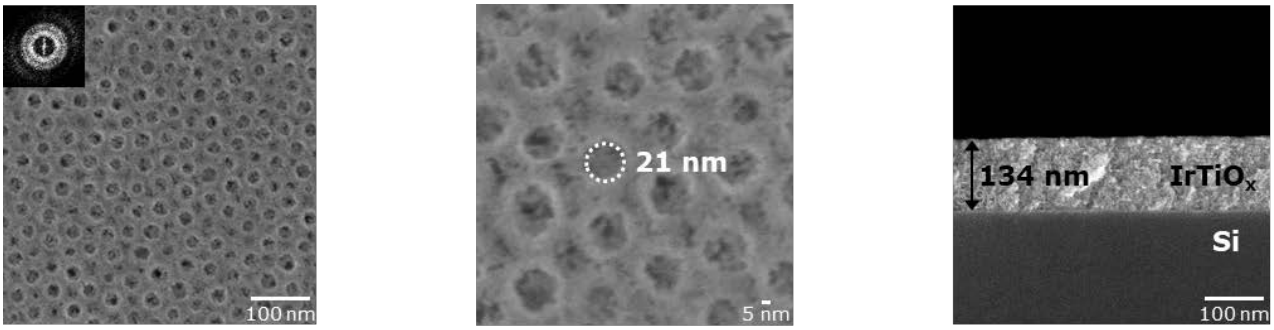

Figure 13: SEM analysis of a mixed oxide layer.

In the case of mixed mesoporous oxide, we now have three target parameters of interest for the functionality of the layer: Apart from the layer **thickness** and the **porosity**, the **elemental composition** of the layer material is of key importance. In this case, the hybrid approach of the layer analysis relies on analysing the layer composition with EDS in a transmission SEM (T-SEM) configuration. Figure 14 illustrates a result of this measurement. Through the EDS method, we have an alternative source for the layer composition and can simultaneously evaluate the layer homogeneity.

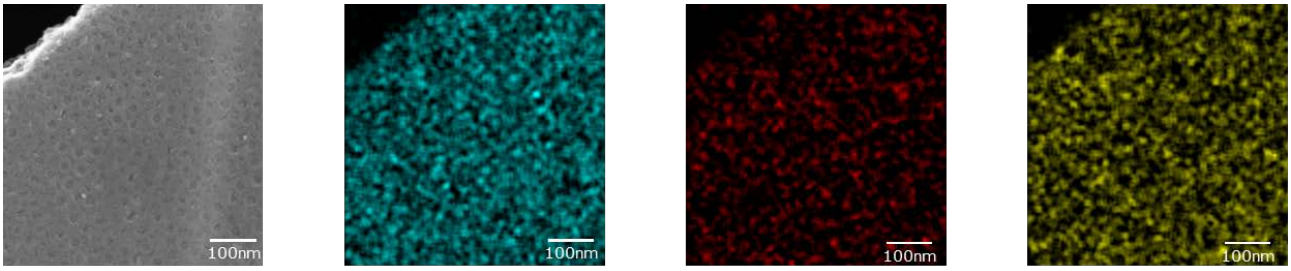

Figure 14: TSEM / EDS analysis of a mixed oxide layer showing imaged of element concentration. From left to right: Grey: TSEM contrast image, EDS elemental distribution maps: Blue: Ti Kα, Red: IrLα, Yellow: O Kα.

Again, we check for the overall validity of the model assumptions by evaluating the comparison of the film thickness obtained from different methods. As can be seen in Figure 15, the agreement is very good and well below a reasonable expectation for the individual uncertainty (see below).

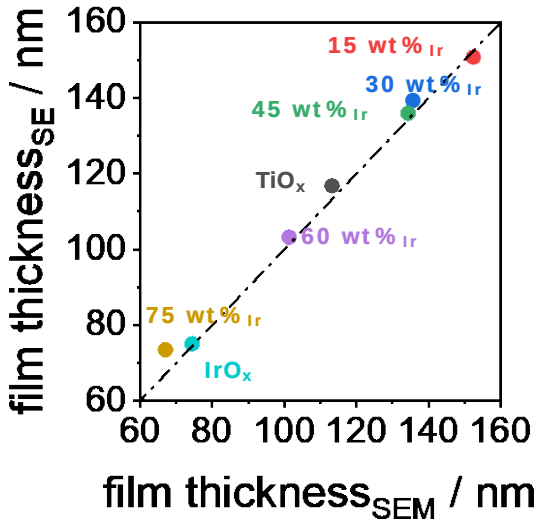

Figure 15: Parity plot comparing the layer thickness from SE with values from SEM.

The same is true to some extent for the Ir content of the layer (Figure 16). There is a very good agreement between the two different chemical composition determination methods (derived from SE and measured by EDS).

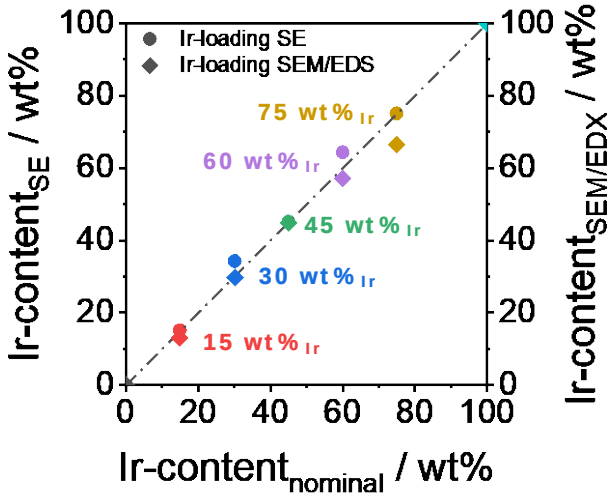

Figure 16: Parity plot comparing the values of the Ir concentration with values obtained from SEM / EDS

Lastly, as shown in Figure 17, we can compare the film porosity values as obtained by different methods. Here, the same problems described earlier becomes obvious. This is a clear sign that the porosity value is in one or more of the methods used here a not very well-quantified parameter and that we must expect the interpretation of data necessary for the calculation of this parameter as challenging (assumed bulk density, stoichiometry, quantification of oxygen, possible in-depth gradients of chemical composition).

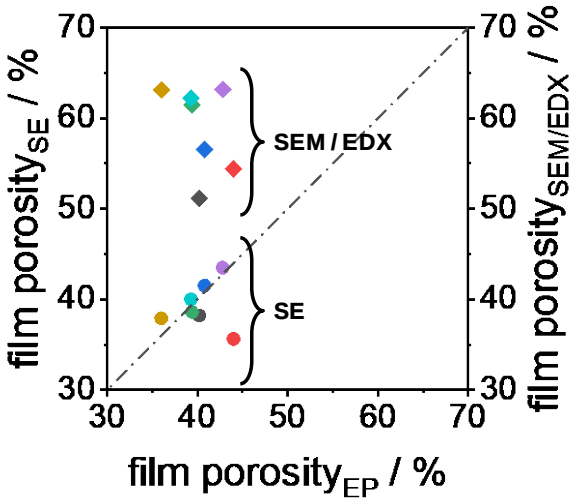

Figure 17: Parity plot comparing the values for the porosity from different methods for mixed oxides.

Considerations on Measurement uncertainty and conclusion

As for all model-based data analysis methods, determining the measurement uncertainty is difficult for ellipsometry as well as for EPMA. The question of accuracy is not purely a calibration or statistical issue, but the methods have an inherent uncertainty from the process of establishing the model. In the present case, we can be very confident not to have obvious errors due to the model lacking important features of the samples. This is proven as the layer thickness determination by SEM which acts as a length calibration. If the models established would be overall wrong, there would be numerous discrepancies in the thickness between the methods. As the determined thickness is practically the same for every sample and with every method, we can be sure that the general properties of the models are correct to a large extent.

The second source of model uncertainty is more difficult to address. It is the coupling of parameters whenever the model used becomes complex [12]. In our case, the models are among the most complex possible in ellipsometry. In recent literature, there has been a development of new methods to quantify the uncertainty resulting from parameter coupling based on statistical sensitivity analysis [9]. Therefore, we use this method developed for a new series of national and international standards [10]. In this last section, we will therefore demonstrate the determination of the model uncertainty due to parameter coupling on the example of a pure TiO_2 layer. The method and its application to this type of layers have been described in detail in [9]. We take in consideration the measurement results depicted before in Figure 8. The RMSE value of this analysis is 66.3. This RMSE value results from a multi-sample analysis covering several samples with different layer thicknesses. However, for this analysis, only one specific thickness is considered as a target parameter. The value for this thickness is 107.2 nm, the porosity is 40.9%. Note that the graph in Figure 8 only contains a very small part of the measured data.

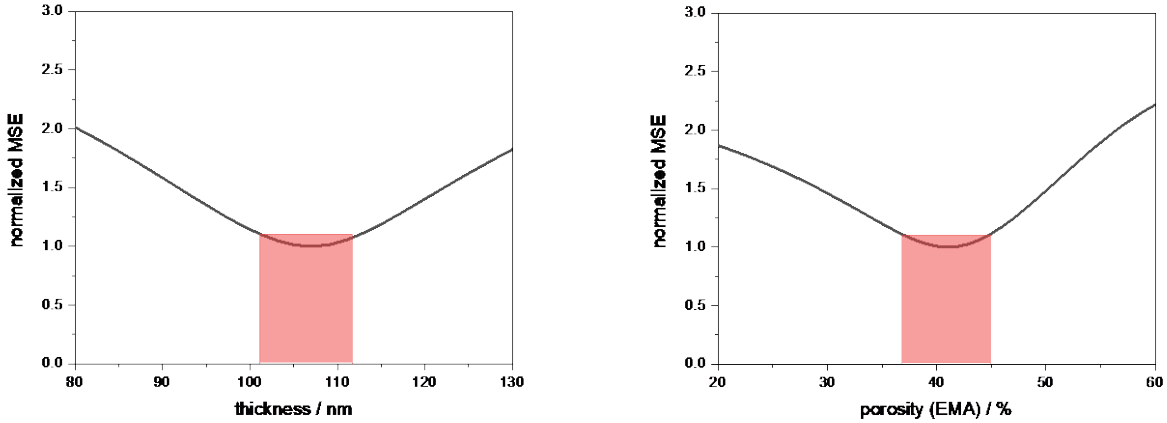

Figure 18: Sensitivity analysis for the ellipsometric analysis of a pure mesoporous TiO_2 layer Left: thickness, right: porosity.

We then identify a small number of target parameters, ideally only one, for which the model uncertainty shall be calculated. Scanning this parameter over a large enough range, while leaving the other parameters free-floating, yields a curve of RMSE over the parameter value. We normalise the RMSE values to their minimum and define a range of confidence as the range this normalised RMSE is lower than 1.1. This is purely an expert's choice which has been well-established in literature. It is expected to give reasonable results for most problems, even as complex as the one present. This produces a rectangular-shaped probability-distribution of the target value which we can then convert to a standard uncertainty compatible with the GUM (Guide to the expression of uncertainty in measurement [13]) which can be included into the standard uncertainty. How to obtain this result is depicted in Figure 18. Note that this contribution is usually much larger than the one coming from the statistical analysis of the fit data that is usually given by the analysis software.

As the last step in this example, we present the full calculation of the uncertainty of the layer thickness. At a value of 107.2 for the layer thickness, the statistical (software uncertainty) is only 0.5 nm. Analysis of the data from Figure 18 gives an uncertainty bandwidth between 99 nm and 114 nm, i.e. 15 nm broad. Converting this to a standard uncertainty (dividing by $\sqrt{3}$ as described in) results in a model uncertainty of 8.7 nm. This is combined linearly with the statistical uncertainty, assuming fully coupled uncertainties ($u = u_{stat} + u_{model}$). The calibration checks on our instrument are performed with a PTB standard of 160 nm thickness with an uncertainty of 0.9 nm as given in the certificate. This is added geometrically ($u = \sqrt{{u_{meas}}^2 + {u_{standard}}^2}$) to the combined uncertainty (assuming decoupled uncertainties) together with the statistical uncertainty of the calibration measurements (0.1 nm). In the end, we obtain a combined uncertainty of 9 nm for the thickness, resulting in an expanded uncertainty of 18 nm (coverage factor of 2). Note, that this (realistic) value is much higher than the precision often denoted to ellipsometry as a measurement technique. We recommend this procedure when communicating results of a multi-parameter analysis.

Conclusion

This guide introduces a possible method for determining highly complex properties of thin layers with a combination methodology of different measurement techniques. It relies on complementary measurement strategies, imaging methods for determining morphology and small scale inhomogeneities. Optical methods with their good properties for production environments, can thus be enabled to be used on even these difficult samples. It is clear, however, that the methodology described here requires a high instrumental effort and expert knowledge. Therefore, this measurement problem should in the long run be solved by the development of reference materials used for the calibration of all techniques involved. This will help to develop further the measurement methods demonstrated in this guide. The long-term goal is to develop production friendly measurement solutions for difficult to analyse nanostructured layers. This follows the idea that new developments in materials and technology, often require accompanying metrology advanced to enable an appropriate quality assurance framework.

References

1. Bernicke, M., et al., *Tailored mesoporous Ir/TiOx: Identification of structure-activity relationships for an efficient oxygen evolution reaction.* Journal of Catalysis, 2019. **376**: p. 209-218.
2. Bernsmeier, D., et al., *Oxygen Evolution Catalysts Based on Ir-Ti Mixed Oxides with Templated Mesopore Structure: Impact of Ir on Activity and Conductivity.* Chemsuschem, 2018. **11**(14): p. 2367-2374.
3. Azzam, R.M.A., *Selected papers on ellipsometry*. SPIE milestone series. 1990, Bellingham, WA: SPIE Optical Engineering Press. xxi, 707 p.
4. Azzam, R.M.A. and N.M. Bashara, *Ellipsometry and polarized light*. 1977, Amsterdam ; New York: North-Holland Pub. Co. ;. xvii, 529 p.
5. Fujiwara, H., *Spectroscopic ellipsometry : principles and applications*. 2007, Chichester, England ; Hoboken, NJ: John Wiley & Sons. xviii, 369 p.
6. Schmidt, D. and M. Schubert, *Anisotropic Bruggeman effective medium approaches for slanted columnar thin films.* Journal of Applied Physics, 2013. **114**(8).
7. Pouchou, J.L., *X-ray microanalysis of thin surface films and coatings.* Mikrochimica Acta, 2002. **138**(3-4): p. 133-152.
8. Ortel, E., et al., *New Approach on Quantification of Porosity of Thin Films via Electron-Excited X-ray Spectra.* Analytical Chemistry, 2016. **88**(14): p. 7083–7090.
9. Rosu, D.M., et al., *Ellipsometric porosimetry on pore-controlled TiO2 layers.* Applied Surface Science, 2017. **421**: p. 487-493.
10. DIN, *DIN 50989-1:2018-03: Ellipsometry - Part 1: Principles; Text in German and English* 2018, Beuth: Berlin.
11. Choi, W.S., et al., *Dielectric constants of Ir, Ru, Pt, and IrO2: Contributions from bound charges.* Physical Review B, 2006. **74**(20).
12. Tompkins, H.G., *A user's guide to ellipsometry*. 2006, Mineola, N.Y.: Dover Publications. xii, 260 p.
13. BIPM and JCGM, *Evaluation of measurement data – Guide to the expression of uncertainty in measurement*. 2008, BIPM: Paris; Available from: https://www.bipm.org/utils/common/documents/jcgm/JCGM_100_2008_E.pdf.